Completeness of Generating Systems for Quadratic Splines on Adaptively Refined Criss-Cross Triangulations

Bert Jüttler, Dominik Mokriš, Urška Zore

Institute of Applied Geometry, Johannes Kepler University, Linz, Austria

Abstract

Hierarchical generating systems that are derived from Zwart-Powell (ZP) elements can be used to generate quadratic splines on adaptively refined criss-cross triangulations. We propose two extensions of these hierarchical generating systems, firstly decoupling the hierarchical ZP elements, and secondly enriching the system by including auxiliary functions. These extensions allow us to generate the *entire* hierarchical spline space – which consists of all piecewise quadratic $\mathcal{C}^1$-smooth functions on an adaptively refined criss-cross triangulation – if the triangulation fulfills certain technical assumptions. Special attention is dedicated to the characterization of the linear dependencies that are present in the resulting enriched decoupled hierarchical generating system.

Keywords: multilevel spline space, criss-cross triangulation, Zwart-Powell elements, completeness
2010 MSC: 65 D07

1. Introduction

We consider spline spaces spanned by Zwart-Powell (ZP) elements, which were originally introduced by Zwart (1973). These functions are compactly supported $\mathcal{C}^1$-smooth piecewise quadratic spline functions defined on criss-cross triangulations, which are also called four-directional grids or type-2 triangulations (Wang, 2001). ZP elements were also recognized as a special instance of box splines, see de Boor et al. (1993) and the references cited therein.

The approximation power of ZP elements has been studied thoroughly in the literature. It was shown by Lyche et al. (2008) that no local quasi-interpolant projector exists for the box spline space defined by translates of the ZP element. Quasi-interpolation operators and the approximation power of ZP elements have been studied by Dahmen and Micchelli (1984), Dagnino and Lamberti (2001) and Foucher and Sablonnière (2008).

Various applications of ZP elements and of the spline spaces generated by them have been described in the literature. These include computer tomography (Entezari et al., 2012; Richter, 1998), computation of isophotes (Aigner et al., 2009), approximation of medial surface transforms (Bastl et al., 2010), generation of offset surfaces (Bastl et al., 2008) and numerical simulation (Kang et al., 2014).

The underlying criss-cross triangulation, which is associated with the ZP elements, possesses a highly regular structure, which precludes the possibility of adaptive refinement. This is similar to the case of tensor-product splines.

Hierarchical splines are one of the main approaches – besides T-splines (Sederberg et al., 2003), PHT-splines (Deng et al., 2008) and LR splines (Dokken et al., 2013) – that were developed to overcome this limitation. Their construction was originally proposed by Forsey and Bartels (1988). About ten years later, Kraft (1997) published a selection mechanism that defines a basis for hierarchial splines and designed a quasi-interpolation operator. Yvart et al. (2005) studied hierarchical triangular splines, whereas Speleers et al. (2009) explored hierarchies of Powell-Sabin splines. Recently, Giannelli et al. (2012) proposed truncated hierarchical B-splines as a modification of Kraft's basis for hierarchical tensor-product splines to restore the partition of unity property without scaling and to improve numerical stability and sparsity properties. Quasi-interpolation operators in this framework were discussed by Speleers and Manni (2016).

The applications reported in the literature include surface fitting and reconstruction (Greiner and Hormann, 1997; Kiss et al., 2014) and isogeometric analysis (Vuong et al., 2011; Schillinger et al., 2012). The idea of truncated hierarchical B-splines has recently been generalized to spaces of functions spanned by generating systems that are possibly linearly dependent (Zore and Jüttler, 2014; Kang et al., 2014). In particular, these studies include the case of ZP elements.

In fact, Kang et al. (2014) in their paper use adaptively refined spaces spanned by hierarchical ZP elements for isogeometric analysis. Their result concerning linear independence (Lemma 4) unfortunately contradicts the related result of Zore and Jüttler (2014) and relies on local linear independence, which is not satisfied by ZP elements, not even after removing one of them to restore linear independence.

The completeness problems for spline spaces is one of the fundamental questions in spline theory. Given a partition of the domain into cells (e.g., a triangulation) and a generating system of smooth piecewise polynomial functions defined on it, does it span the entire spline space consisting of the piecewise polynomial functions with a specified order of smoothness? It is closely related to the computation of the dimension of a spline space. See the monographs of Lai and Schumaker (2007) and Wang (2001) for a detailed introduction.

Several approaches to answer the completeness question and to compute the dimension have been proposed in the literature. The very powerful approach of

using techniques from homological algebra was introduced by Billera (1988) and has been further explored since, e.g., by Mourrain (2014) and Schenck and Stillman (1997). The important particular case of biquadratic splines on hierarchical T-meshes has been extensively studied using the smoothing cofactor method (e.g., Huang et al., 2006; Zeng et al., 2015), and similar results are available for higher degrees as well. Indeed, the case of tensor-product splines of general degree on hierarchical meshes has attracted particular attention due to the importance for applications.

Homological techniques for hierarchical tensor-product splines were used by Berdinsky et al. (2014, 2015). The characterization of the contact of polynomials via blossoming led to the results by Mokriš et al. (2014) and Mokriš and Jüttler (2014). These generalize the earlier results of Giannelli and Jüttler (2013) on bivariate splines to the full multivariate case.

The present paper extends the latter approach to the case of bivariate splines on adaptively refined criss-cross triangulations, which are obtained by collecting triangles from a hierarchy of nested criss-cross triangulations. The case of triangulations with only one level is studied in Section 2. Considering triangles from criss-cross triangulations of several levels simultaneously leads us to the definition of the multilevel spline space, which is formalized in Section 3.

Since ZP elements are defined on each of the criss-cross triangulations that form the hierarchy, it is natural to produce a generating system by selecting ZP elements of the different levels using a suitably modified version of Kraft's construction. In order to achieve completeness of this generating system, and to control its linear dependencies, we propose to decouple the ZP elements and to enrich the hierarchical generating system by additional functions, see Section 4. Suitably generalizing the techniques of Giannelli and Jüttler (2013) then enables us to establish the completeness property under certain technical assumptions in Section 5 and to analyze the resulting linear dependencies in Section 6.

2. Zwart-Powell elements on multicell domains

After reviewing some well-known facts about Zwart-Powell box splines, we show that their restrictions span the entire space of $\mathcal{C}^1$–smooth quadratic splines on a multicell domain.

We consider the points lying on horizontal, vertical and diagonal lines

$$x = 2^{-\ell} i \;\text{ or }\; y = 2^{-\ell} i \;\text{ or }\; x + y = 2^{-\ell} i \;\text{ or }\; x - y = 2^{-\ell} i, \quad i \in \mathbb{Z},$$

which form a four-directional grid $\mathcal{G}^\ell$ in the plane $\mathbb{R}^2$. Varying the integer ℓ, which is called the *level*, leads to dyadic refinement and coarsening of the grid. While we keep it constant in this section (choosing, e.g., $\ell = 1$), we shall consider grids of different levels in the later part of the paper.

The closures of the connected components of $\mathbb{R}^2 \setminus \mathcal{G}^\ell$ are called the *cells*, and the set formed by them will be denoted by C^ℓ. Any subset thereof is called a *criss-cross triangulation* of level ℓ, see Fig. 1. More precisely, we shall speak of a criss-cross triangulation of the domain that is covered by these triangles; often we will omit the information about the level if it is clear from the context.

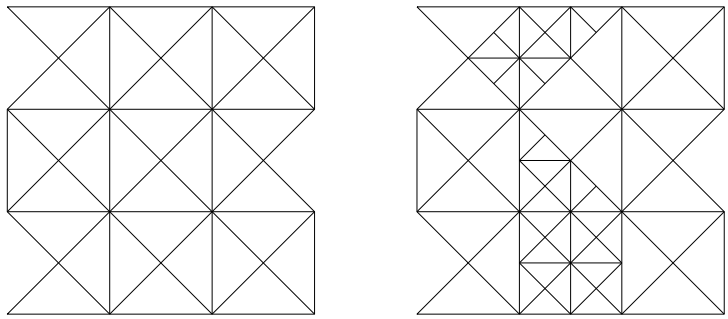

Figure 1: Left: criss-cross triangulation; Right: triangulation, which is not a criss-cross triangulation.

More generally, any set Δ of triangles in $\mathbb{R}^2$ with mutually disjoint interiors is called a *triangulation*. The *union operator* $U(\Delta)$, which is defined by

$$U(\Delta) = \bigcup_{c \in \Delta} c,$$

transforms each triangulation into a planar domain covered by its triangles.

If $\Delta^\ell \subset C^\ell$ is a criss-cross triangulation of level ℓ, then the set $D^\ell = U(\Delta^\ell) \subset \mathbb{R}^2$ shall be called a *multicell domain of level* ℓ. Clearly it is then also a multicell domain of any level ℓ' larger than ℓ, as we consider nested grids.

Conversely, the *triangulation operator* T^ℓ of level ℓ, which is defined by

$$T^\ell(D) = \{c \in C^\ell \mid c \subseteq D\},$$

transforms any set $D \subseteq \mathbb{R}^2$ into the maximal criss-cross triangulation covered by it. We omitted the upper index ℓ of D since T^ℓ can be applied to any set.

When applied to criss-cross triangulations Δ^ℓ and multicell domains D^ℓ of level ℓ, the union and triangulation operators are inverses of each other,

$$T^\ell(U(\Delta^\ell)) = \Delta^\ell \quad \text{and} \quad U(T^\ell(D^\ell)) = D^\ell.$$

For any criss-cross triangulation Δ^ℓ of level ℓ we will denote the associated multicell domain of level ℓ by D^ℓ and vice versa.

Additionally, we introduce the *splitting operator* S, which transforms each set $D \subseteq \mathbb{R}^2$ into the set $S(D)$ that is formed by its maximal connected components,

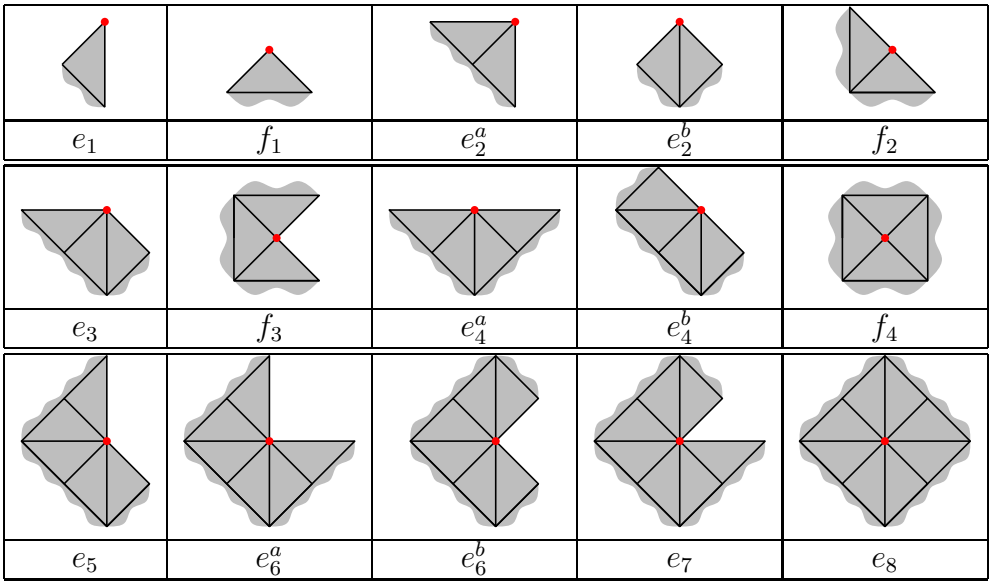

Table 1: Classification of vertices (red dots) of a triangulation without kissing vertices.

i.e.,

$$D = \dot{\bigcup_{k \in S(D)}} k,$$

where each k is a connected subset of D that is not contained in any other connected subset of D.

We now classify the vertices which are contained in a multicell domain D^ℓ. A regular vertex is characterized by the fact that D^ℓ is a topological manifold with boundary in its sufficiently small neighborhood. Each regular vertex belongs to one of the types schematically shown in Table 1 (up to rotations by integer multiples of $\pi/2$ and reflections). The symbols shown below denote the number of vertices of the particular type, where e and f stands for vertices of valence 8 and 4 in the underlying grid and the lower index specifies the number of incident triangles. We omit the index ℓ to simplify the notation.

The remaining vertices will be called *kissing vertices*. Based on their valence with respect to the underlying grid, they will be called *valence-4 kissing vertices* and *valence-8 kissing vertices*, respectively. An example is shown in Fig. 2. Note that the valence does not refer to the criss-cross triangulation of D^ℓ but to the underlying grid. There is only one possible type of a valence-4 kissing vertex, while several types of valence-8 kissing vertices exist, see Fig. 2.

Definition 1. We define the *spline space of degree d and smoothness r on a triangulation* Δ by

$$\mathbb{S}_d^r(\Delta) = \{\sigma \in \mathcal{C}^r(U(\Delta)) \mid \forall c \in \Delta : \sigma|_c \in \mathbb{P}_d|_c\}, \tag{1}$$

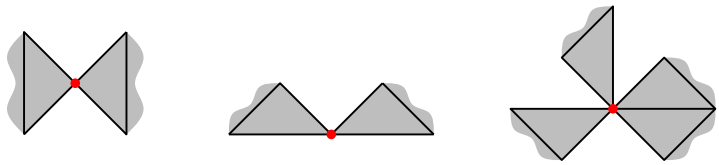

Figure 2: From left to right: the only type of a valence-4 kissing vertex and two examples of a valence-8 kissing vertex.

where $\mathbb{P}_d|_c$ is the space of polynomials of degree d restricted to the triangle c.

In this definition, we use $\mathcal{C}^r(F)$ to denote the space of all functions defined on $F \subset \mathbb{R}^2$ that possess continuous partial derivatives up to order r in the interior of F and which can be continuously extended to the closure $\overline{F}$. Consequently, the spline space (1) is well defined even for multicell domains where kissing vertices are present.

In the remainder of this section, we analyze the dimension of the spline space $\mathbb{S}_2^1(\Delta^\ell)$ on a criss-cross triangulation Δ^ℓ of level ℓ.

Lemma 2. *If Δ^ℓ does not contain any kissing vertices, then*

$$\dim \mathbb{S}_2^1(\Delta^\ell) = 6 + e_8 + \frac{1}{2}\left(\sum_{i=1}^{7}(i-1)v_i - 3f_4\right) \tag{2}$$

with $e_i = e_i^a + e_i^b$ for $i \in \{2,4,6\}$ and $v_i = e_i + f_i$, where all undefined quantities are equal to zero, e.g., $f_5 = 0$.

Proof. The term in the parentheses in (2) counts the incident inner edges of all boundary vertices. This equals twice the number of the *cross-cuts* of Δ^ℓ, which are the line segments that intersect the boundary of D^ℓ exactly in their end points. The formula (2) is then a special case of (Wang, 2001, Theorem 2.2). □

For each $\mathbf{i} \in \mathbb{Z}^2$ we define the *Zwart-Powell (ZP) element* $\zeta_{\mathbf{i}}^\ell$ on the level ℓ criss-cross triangulation by its Bernstein-Bézier coefficients as shown in Fig. 3. The center of the support of such an element is the point $2^{-\ell}(\mathbf{i} + (\frac{1}{2}, \frac{1}{2}))$.

For each ZP element $\zeta_{\mathbf{i}}^\ell$ and a domain $D \subseteq \mathbb{R}^2$ we define *support components* $S(\operatorname{supp} \zeta_{\mathbf{i}}^\ell \cap D)$ as the connected components of the support of the restricted function $\zeta_{\mathbf{i}}^\ell|_D$. Note that we take

$$\operatorname{supp} f(\mathbf{x}) = \{\mathbf{x} \in \mathbb{R}^2 \mid f(\mathbf{x}) \neq 0\}$$

and, therefore, in the case of ZP elements, the support is an *open* set. Note also that in case of a kissing vertex, one has to take special care: such a vertex may

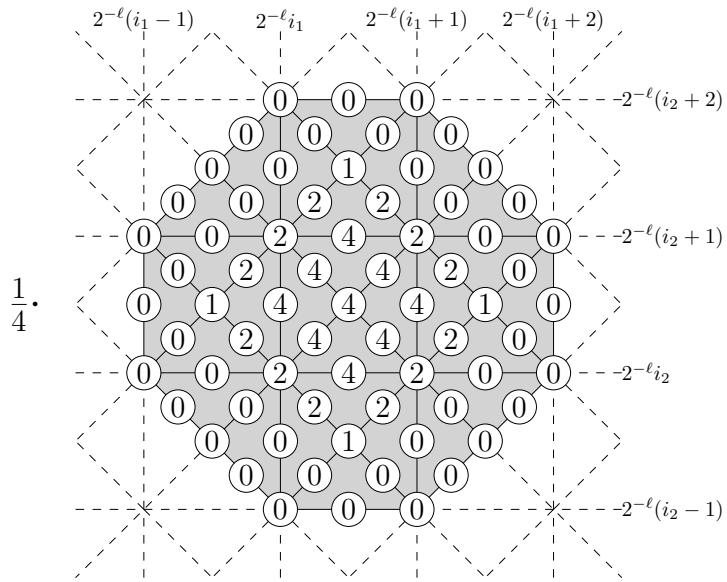

Figure 3: Bernstein-Bézier coefficients defining a ZP element.

split $\operatorname{supp}\zeta_{\mathbf{i}}^{\ell} \cap D$ into several connected components only if it is on the boundary of the octagon $\operatorname{supp}\zeta_{\mathbf{i}}^{\ell}$. An example is shown in Fig. 4.

Since we will need to refer to the support components for the different ZP elements, we introduce the index set

$$I_D^{\ell} = \bigcup_{\mathbf{i}\in\mathbb{Z}^2} \{\mathbf{i}\} \times S(\operatorname{supp}\zeta_{\mathbf{i}}^{\ell} \cap D),$$

which consists of pairs $\hat{\boldsymbol{\imath}} = (\mathbf{i}, s)$ where s is a support component of $\zeta_{\mathbf{i}}^{\ell}$.

Definition 3. The *separated generating system* $R_D^{\ell} = \{\varrho_{\hat{\boldsymbol{\imath}}}^{\ell} \mid \hat{\boldsymbol{\imath}} \in I_D^{\ell}\}$ on a domain $D \subseteq \mathbb{R}^2$ is formed by the restrictions of the ZP elements to their support components (each considered separately)

$$\varrho_{(\mathbf{i},s)}^{\ell}(\mathbf{x}) = \begin{cases} \zeta_{\mathbf{i}}^{\ell}(\mathbf{x}) & \text{if } \mathbf{x} \in s, \\ 0 & \text{otherwise.} \end{cases}$$

These are indexed by $\hat{\boldsymbol{\imath}} = (\mathbf{i}, s) \in I_D^{\ell}$.

Note that the restriction of a ZP element to D is decomposed into *separated ZP elements*

$$\sum_{s\in S(\operatorname{supp}\zeta_{\mathbf{i}}^{\ell}\cap D)} \varrho_{(\mathbf{i},s)}^{\ell}(\mathbf{x}) = \zeta_{\mathbf{i}}^{\ell}(\mathbf{x}) \text{ for } \mathbf{x} \in D. \tag{3}$$

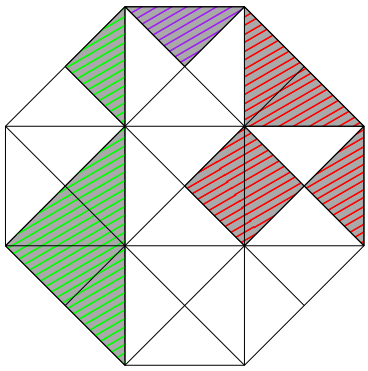

Figure 4: The kissing vertices of the multicell domain (shown in gray) split the support of the element (the outer octagon) into several components shown in tiling of various colors (red, blue and green). Note that the connected component shown in red is indeed connected due to the kissing vertices inside the support.

The sum is empty if no support component exists. It consists of one or more contributions otherwise.

Lemma 4. *If $D = c$ is a single cell of level ℓ, then R_c^ℓ consists of seven functions and any six of them are linearly independent.*

Proof. This can be confirmed by a direct computation using the Bernstein-Bézier representations of the ZP elements, see Fig. 3. The seven local coefficient vectors form the matrix

$$\begin{pmatrix} 2 & 0 & 0 & 0 & 0 & 0 \\ 2 & 2 & 1 & 2 & 2 & 4 \\ 0 & 0 & 0 & 0 & 2 & 0 \\ 0 & 0 & 1 & 2 & 2 & 0 \\ 2 & 4 & 4 & 4 & 2 & 4 \\ 2 & 2 & 1 & 0 & 0 & 0 \\ 0 & 0 & 1 & 0 & 0 & 0 \end{pmatrix}$$

and removing any row thereof produces a regular matrix. □

We extend this observation to connected multicell domains.

Lemma 5. *Removing at least one function from $R_{D^\ell}^\ell$ produces a linearly independent system if D^ℓ is a connected multicell domain of level ℓ.*

Proof. After removing at least one function, we obtain a subset $R' \subsetneq R_{D^\ell}^\ell$. We consider a linear combination of the zero function by functions in R' with certain coefficients. The difference $R_{D^\ell}^\ell \setminus R'$ contains one or more functions and we consider all cells c in their combined support. The previous lemma implies that the coefficients of all functions in R' with a support containing at least one of these cells are equal to zero. Adding these functions to the difference set then increases

the number of cells in the combined support since D^ℓ is connected, unless the cells already cover D^ℓ entirely. Using the same argument repeatedly shows that all coefficients are equal to zero. $\square$

The coefficients

$$\chi_{\hat{\boldsymbol{\imath}}} = \chi_{(\mathbf{i},s)} = (-1)^{(i_1+i_2)}$$

will be called the *chessboard pattern*. Note that their values are independent of s.

Lemma 6. *Any representation*

$$0 = \sum_{\hat{\boldsymbol{\imath}} \in I^\ell_{D^\ell}} \alpha_{\hat{\boldsymbol{\imath}}} \varrho^\ell_{\hat{\boldsymbol{\imath}}}(\mathbf{x}) \tag{4}$$

of the zero function on a connected multicell domain D^ℓ of level ℓ has coefficients of the form $\alpha_{\hat{\boldsymbol{\imath}}} = \lambda \chi_{\hat{\boldsymbol{\imath}}}$ for some scalar λ.

Proof. A direct computation using the Bernstein-Bézier representation (see Fig. 3) confirms

$$0 = \sum_{\hat{\boldsymbol{\imath}} \in I^\ell_{D^\ell}} \chi_{\hat{\boldsymbol{\imath}}} \varrho^\ell_{\hat{\boldsymbol{\imath}}}(\mathbf{x}). \tag{5}$$

Consequently, any function $\varrho^\ell_{\hat{\boldsymbol{\imath}}'}$ with $\hat{\boldsymbol{\imath}}' \in I^\ell_{D^\ell}$ can be represented as a linear combination

$$\varrho^\ell_{\hat{\boldsymbol{\imath}}'} = - \sum_{\hat{\boldsymbol{\imath}} \in I^\ell_{D^\ell} \setminus \{\hat{\boldsymbol{\imath}}'\}} \frac{\chi_{\hat{\boldsymbol{\imath}}}}{\chi_{\hat{\boldsymbol{\imath}}'}} \varrho^\ell_{\hat{\boldsymbol{\imath}}} \tag{6}$$

of the remaining functions. Given an identity of the form (4), using the representation (6) of the function $\varrho^\ell_{\hat{\boldsymbol{\imath}}'}$ transforms it into a linear combination of functions in $R^\ell_{D^\ell} \setminus \{\varrho^\ell_{\hat{\boldsymbol{\imath}}'}\}$ with coefficients

$$\alpha_{\hat{\boldsymbol{\imath}}} - \underbrace{\frac{\alpha_{\hat{\boldsymbol{\imath}}'}}{\chi_{\hat{\boldsymbol{\imath}}'}}}_{=\lambda} \chi_{\hat{\boldsymbol{\imath}}}.$$

These coefficients are equal to zero, as the functions are linearly independent according to Lemma 5. This completes the proof. $\square$

Note that any two functions $\varrho^\ell_{(\mathbf{i},s)}$ and $\varrho^\ell_{(\mathbf{i},s')}$ that are derived from the same function $\zeta^\ell_{\mathbf{i}}$ (see Definition 3) are multiplied by the same coefficient $\lambda\chi_{\hat{\boldsymbol{\imath}}}$ in (4).

Definition 7. A multicell domain D^ℓ is *admissible*, if its connected components are simply connected and no valence-4 kissing vertices are present in $T^\ell(D^\ell)$.

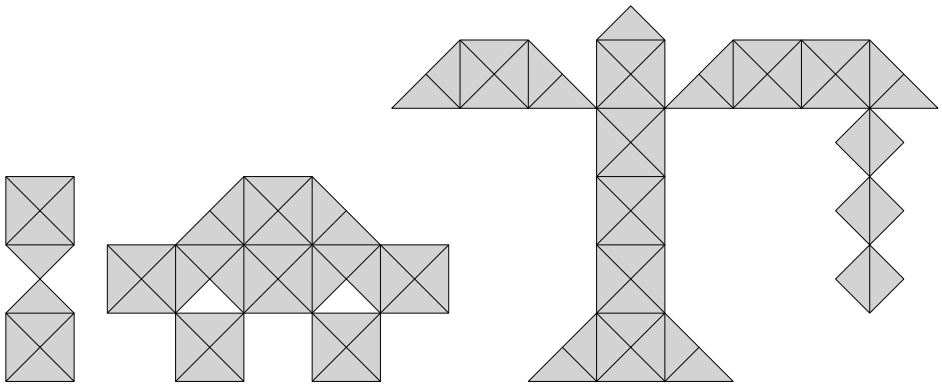

Figure 5: Admissible (right) and non-admissible (left and center) multicell domains.

Definition 7 rules out multicell domains with holes. Some admissible and non-admissible level ℓ multicell domains are presented in Fig. 5.

Theorem 8. *If D^ℓ is an admissible multicell domain of level ℓ, then the separated generating system on its criss-cross triangulation Δ^ℓ of level ℓ is complete, i.e.,*

$$\operatorname{span}\{\varrho^\ell_{\hat{\boldsymbol{\imath}}} \mid \hat{\boldsymbol{\imath}} \in I^\ell_{D^\ell}\} = \mathbb{S}^1_2(\Delta^\ell). \tag{7}$$

Proof. The proof consists of two steps: Firstly, we prove the theorem in the case of a single connected component without kissing vertices, based on the dimension result (2). Secondly, we extend it to domains with valence-8 kissing vertices and several connected components.

Step 1. We consider a simply connected domain without kissing vertices. According to Lemma 5 it suffices to prove that

$$\dim \mathbb{S}^1_2(\Delta^\ell) = |I^\ell_{D^\ell}| - 1. \tag{8}$$

A careful case-by-case analysis, which is similar to the offset counting by Mokriš et al. (2014), leads to

$$\begin{aligned} |I^\ell_{D^\ell}| &= |\{\varrho^\ell_{\hat{\boldsymbol{\imath}}} \mid \hat{\boldsymbol{\imath}} \in I^\ell_{D^\ell}\}| \\ &= 2e_1 + 2f_1 + e_2^a + 2e_2^b + f_2 + e_3 + e_4^b + f_4 - e_6^a - 2e_7 + \varepsilon_b, \end{aligned} \tag{9}$$

where ε_b is the number of axis-aligned (i.e., horizontal or vertical) boundary edges. Substituting (9) and (2) into (8) results (after rewriting) in the equivalent formula

$$\begin{aligned} 2\varepsilon_b + 4e_1 + 4f_1 + e_2^a + 3e_2^b + f_2 - 2f_3 - 3e_4^a - e_4^b + 2f_4 \\ - 4e_5 - 7e_6^a - 5e_6^b - 8e_7 - 2e_8 - 14 = 0, \end{aligned} \tag{10}$$

which is now proved with the help of four identities:

(i) Each axis-aligned boundary edge has two incident vertices and each boundary vertex has between zero and two incident axis-aligned boundary edges, depending on its type, thus

$$2\varepsilon_b = e_1 + 2e_2^a + e_3 + 2e_4^a + e_5 + 2e_6^a + e_7.$$

(ii) Each non-axis-aligned (i.e., diagonal) boundary edge connects one vertex of valence 4 with one vertex of valence 8, and each boundary vertex has between zero and two incident non-axis-aligned boundary edges. Counting the contributions of the boundary vertices of the two different valencies separately gives

$$2f_1 + 2f_2 + 2f_3 = e_1 + 2e_2^b + e_3 + 2e_4^b + e_5 + 2e_6^b + e_7.$$

(iii) A similar observation, applied to the interior non-axis-aligned edges gives

$$f_2 + 2f_3 + 4f_4 = e_2^a + e_3 + 2e_4^a + e_4^b + 2e_5 + 3e_6^a + 2e_6^b + 3e_7 + 4e_8.$$

(iv) The boundary of the domain is a simple closed curve, hence the total turning of the tangent vector equals 2π. Summing up the turning angles for the different types of boundary vertices confirms that

$$(3e_1 + 2f_1 + 2e_2^a + 2e_2^b + e_3 - 2f_3 - e_5 - 2e_6^a - 2e_6^b - 3e_7)\frac{\pi}{4} = 2\pi.$$

A suitable linear combination of the four identities (i-iv) proves Eq. (10), which is equivalent to (8).

Step 2. First we extend our result to simply connected domains with valence-8 kissing vertices. Such a domain can be subdivided at the kissing vertices into several simply connected parts. (For instance, the domain in Fig. 5 (right) is subdivided into 6 connected parts without kissing vertices.) Any function in $\mathbb{S}_2^1(\Delta^\ell)$, which is defined on the entire domain, can be represented as a linear combination of the functions in the separated generating system on each of these parts. Clearly, each of these representations can be modified by adding a real multiple of the chessboard pattern, since the coefficients thereof correspond to the zero function.

We number the parts, starting with 1, so that each part is connected by a kissing vertex to exactly one part with a lower number, except for the first one. At each kissing vertex, exactly four functions in each of the separated generating systems on the parts joining there take non-zero values. We visit the parts according to the chosen ordering and add a scaled multiple of the chessboard pattern to make sure that one of the four associated coefficients takes the same value. Since the function is $\mathcal{C}^1$-smooth at the kissing vertex, the remaining three coefficients take the same

values too, as there are three equations characterizing a $\mathcal{C}^1$-joint at the kissing vertex. This completes the proof for simply connected domains with valence-8 kissing vertices.

Finally, we note that, since the support components are considered separately, the theorem extends to admissible domains with more than one connected component, as the representations on the different components are independent of each other. $\square$

Theorem 8 does not generalize to domains possessing valence-4 kissing vertices, since there are five functions in each of the separated generating systems on the parts joining there that take non-zero values. Moreover, the theorem is not valid for non-admissible domains, as demonstrated by the following example.

Example 9. We consider the level 0 multicell domain D^0 shown in Fig. 6 (left), which is not admissible in the sense of Definition 7. Removing the dashed line segment AB transforms it into a simply connected domain. The dimension of the spline space defined on that domain is equal to 41 according to Lemma 2. Enforcing $\mathcal{C}^1$-smoothness across AB reduces the dimension of the space by 5, therefore $\dim \mathbb{S}_2^1(\Delta^0) = 36$. The number of linearly independent functions in the separated generating system, however, amounts to 35 only. Consequently this system does not generate the entire spline space on D^0.

The construction of a function in $\mathbb{S}_2^1(\Delta^0) \setminus \operatorname{span} R_{D^0}^0$ is shown in Fig. 6 (right). The function is equal to zero everywhere except in the green region. Within that region, the function is defined as a linear combination of the six ZP elements with the coefficients specified in the picture. Due to the choice of these coefficients as a subset of a chessboard pattern, the function is $\mathcal{C}^1$-smooth and therefore belongs to $\mathbb{S}_2^1(\Delta^0)$. However, it does not admit a representation by ZP elements of level 0.

Indeed, this function can be represented as a linear combination of 42 ZP elements on the simply connected domain obtained after removing AB, where only six coefficients (the ones shown in the figure) take non-zero values. These six coefficients correspond to the six ZP elements that are split into pairs of separated functions, and the non-zero coefficients are assigned to the separated functions that act on the right-hand side of AB. This representation on the simply connected domain is unique up to additions of multiples of the chessboard pattern. However, no addition of such a multiple gives a representation with the property that the six pairs of coefficients of the separated ZP elements possess matching values. $\diamond$

3. Hierarchical spline spaces

In the remainder of the paper we consider criss-cross triangulations of several levels and the ZP elements defined on them simultaneously. An adaptively refined spline space is defined with the help of a hierarchy of subdomains.

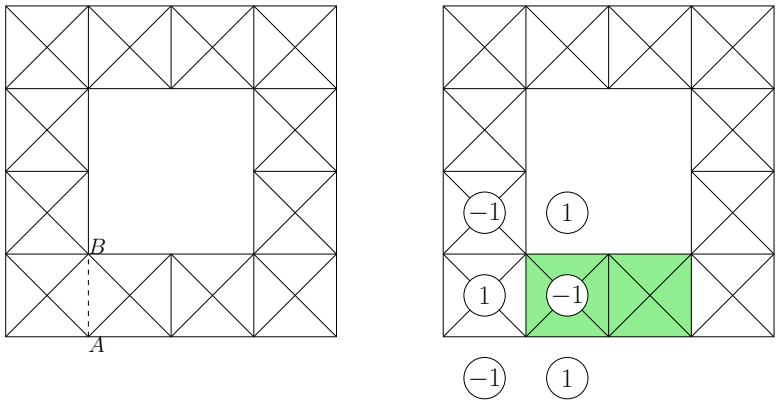

Figure 6: Left: A non-admissible multicell domain of level 0 with an incomplete separated generating system. Right: A function in $\mathbb{S}_2^1(\Delta^0)$ that cannot be represented by the separated generating system.

More precisely, given a bounded domain $\Omega^0 \subset \mathbb{R}^2$, the definition of a hierarchical spline space is based on a nested sequence of $N+1$ subdomains

$$\Omega^0 \supseteq \Omega^1 \supseteq \cdots \supseteq \Omega^{N-1} \supseteq \Omega^N = \emptyset,$$

where N denotes the number of levels in the hierarchy. Setting $\Omega^N = \emptyset$ simplifies some of the definitions below.

Each subdomain Ω^ℓ represents the part of Ω^0 selected for refinement to functions of level ℓ, in order to benefit from the increased approximation properties in this region.

We will assume that each *difference set*

$$D^\ell = \overline{\Omega^0 \setminus \Omega^{\ell+1}},\ \ell = -1, \ldots, N-1,$$

is a multicell domain of level ℓ. This is automatically satisfied if each $\Omega^{\ell+1}$ is a multicell domain of level ℓ. In particular, we have that $D^{-1} = \emptyset$ and $D^{N-1} = \Omega^0$.

Definition 10. The spline space $\mathbb{H} = \mathbb{S}_2^1(\Delta_H)$, which is defined on the adaptively refined triangulation

$$\Delta_H = \bigcup_{\ell=0}^{N-1} T^\ell(\overline{\Omega^\ell \setminus \Omega^{\ell+1}}),$$

will be called the *multilevel spline space*.

The adaptively refined triangulation Δ_H is obtained by triangulating each set $\Omega^\ell \setminus \Omega^{\ell+1}$ individually using cells of level ℓ. Combining these gives a triangulation of the entire domain Ω^0, possibly with cells of different levels. The individual triangulations are obtained by applying the triangulation operator T^ℓ from Section 2.

The following equivalent characterization of the multilevel spline space will be useful.

Lemma 11. *The multilevel spline space can be equivalently characterized by*

$$\mathbb{H}' = \{\sigma : \Omega^0 \to \mathbb{R} \mid \forall_{\ell=0}^{N-1} : \sigma|_{D^\ell} \in \mathbb{S}_2^1(\Delta^\ell)\},$$

i.e., $\mathbb{H} = \mathbb{H}'$.

Proof. On the one hand, the inclusion $\mathbb{H} \subseteq \mathbb{H}'$ follows from the fact that Δ^ℓ is a finer triangulation of the domain covered by

$$\bigcup_{k=0}^{\ell} T^k(\overline{\Omega^k \setminus \Omega^{k+1}})$$

for $\ell = 0, \ldots, N-1$. On the other hand, any spline function $\sigma \in \mathbb{H}'$ is $\mathcal{C}^1$-smooth on Ω^0 since $U(\Delta^{N-1}) = D^{N-1} = \Omega^0$. Moreover, it is a single polynomial on each triangle in Δ_H. Indeed, for each $c \in \Delta_H$ there exists a level ℓ such that $c \in \Delta^\ell$ and $\sigma \in \mathbb{S}_2^1(\Delta^\ell)$. We conclude that $\sigma \in \mathbb{S}_2^1(\Delta_H) = \mathbb{H}$. □

The next section proposes a generating system for the multilevel spline space. An affirmative answer to the completeness question will be given later in Section 5.

4. Enriched decoupled hierarchical generating systems

We introduce decoupled Zwart-Powell elements and auxiliary functions, which we will call partial chessboard functions. The enriched decoupled hierarchical generating system is then constructed using a selection procedure which is inspired by the work of Kraft (1997).

It should be noted that we use a slightly modified definition of the support in the remainder of the paper. Since the domain of all functions under consideration is the set Ω^0 introduced in Section 3, all supports are understood as subsets thereof, i.e.,

$$\operatorname{supp}^0 f = \{\mathbf{x} \in \Omega^0 \mid f(\mathbf{x}) > 0\}.$$

The grids of adjacent levels are nested, $\mathcal{G}^\ell \subset \mathcal{G}^{\ell+1}$. Each ZP element of level ℓ can be represented as a linear combination of 12 elements of level $\ell + 1$ with the coefficients shown in Fig. 7. Consequently, the space generated by the ZP elements

$$Z^\ell = \{\zeta_{\mathbf{i}}^\ell \mid \mathbf{i} \in \mathbb{Z}^2\}$$

of level ℓ is a refinement of the coarser space spanned by the elements of the coarser levels. Raising the level ℓ increases the approximation power, see Foucher and Sablonnière (2008).

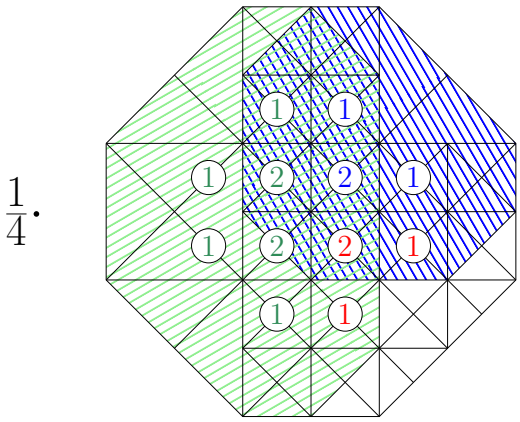

Figure 7: Refinement coefficients of the 12 ZP elements obtained by representing the element at the next level, and the supports of two decoupled functions obtained from it.

In Section 2, we introduced the separated generating systems by considering the support components of the ZP elements with a given multicell domain D^ℓ. This system, however, consists of functions that are defined on D^ℓ only. We will now use the refinability of ZP elements to construct *decoupled* functions that continuously extend the separated ones to $\mathbb{R}^2$. In order to do so, we need an assumption, which we call the *support intersection condition* (SIC):

$$\forall_{\ell=0}^{N-2}\ \forall \mathbf{i} \in \mathbb{Z}^2 \ :\ \operatorname{supp}^0 \zeta_{\mathbf{i}}^{\ell+1} \cap D^\ell \text{ is connected.} \tag{SIC}$$

This condition is illustrated in Fig. 8, which shows several hierarchical grids consisting of two levels $\ell = 0, 1$ and the support of ZP elements of level 1 (hatched). The set D^0 consists of all cells that belong to the coarser grid. SIC is satisfied for the first two triangulations (left and center) since the support components with D^0 are all connected, while this is not the case for the third one (right).

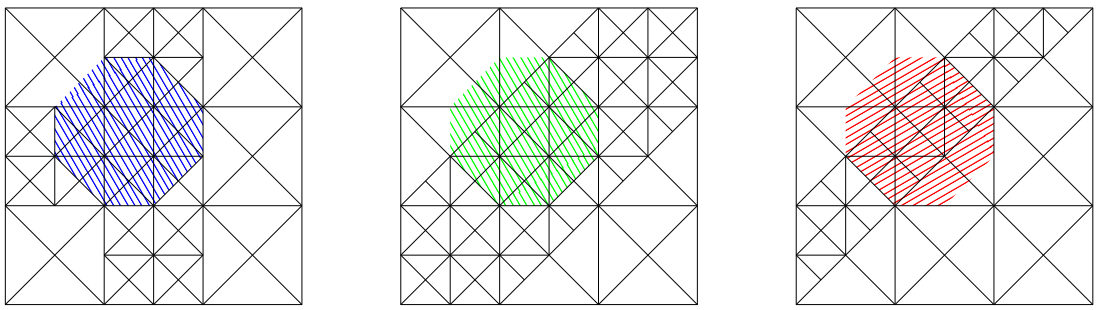

Figure 8: Adaptively refined triangulations with two levels satisfying (left and center) and violating (right) SIC. The supports of ZP elements on the finer grid are hatched.

SIC is automatically satisfied if each triangulation $T(D^\ell)$ possesses no vertices

of type f_1, f_2 and f_3, i.e., the multicell domains D^ℓ consist of squares formed by the four triangles incident to vertices of type f_4, see again Fig. 8 left.

Definition 12. For each index $\hat{\boldsymbol{\imath}} = (\mathbf{i}, s) \in I^\ell_{D^\ell}$ we define the *decoupled function*

$$\gamma^\ell_{\hat{\boldsymbol{\imath}}} = \gamma^\ell_{(\mathbf{i},s)} = \sum_{\{\mathbf{j} \mid \operatorname{supp}^0 \zeta^{\ell+1}_{\mathbf{j}} \cap s \neq \emptyset\}} c_{\mathbf{i},\mathbf{j}} \zeta^{\ell+1}_{\mathbf{j}}, \tag{11}$$

where the coefficients $c_{\mathbf{i},\mathbf{j}}$ are determined by representing the ZP element $\zeta^\ell_{\mathbf{i}}$ with respect to the ZP elements of the next finer level, i.e.,

$$\zeta^\ell_{\mathbf{i}} = \sum_{\mathbf{j} \in \mathbb{Z}^2} c_{\mathbf{i},\mathbf{j}} \zeta^{\ell+1}_{\mathbf{j}}, \tag{12}$$

using the refinement relation shown in Fig. 7. All decoupled functions of level ℓ form the set G^ℓ.

Note that $\operatorname{supp}^0 \zeta^\ell_{\mathbf{i}} \subseteq D^\ell$ implies $\gamma^\ell_{\hat{\boldsymbol{\imath}}} = \zeta^\ell_{\mathbf{i}}$ where $\hat{\boldsymbol{\imath}} = (\mathbf{i}, \operatorname{supp}^0 \zeta^\ell_{\mathbf{i}})$.

The construction of decoupled functions is visualized in Fig. 7. A ZP element of level 0, whose support is the entire octagon, is used to define two decoupled functions according to (11). This element possesses two support components. The ZP element is represented as a linear combination of 12 ZP elements of level 1 with coefficients shown in the circles, which are then grouped according to the associated support components. The green and blue coefficients correspond to the left and the upper right support component. The supports of the elements associated with the red coefficients do not intersect D^0. Consequently, we obtain two decoupled functions in this case, the supports of which (hatched regions) are shown in green and blue.

Lemma 13. *SIC implies that the decoupled functions satisfy*

$$\gamma^\ell_{\hat{\boldsymbol{\imath}}}(\mathbf{x}) = \varrho^\ell_{\hat{\boldsymbol{\imath}}}(\mathbf{x}) \text{ for all } \mathbf{x} \in D^\ell.$$

Therefore, $G^\ell|_{D^\ell} = R^\ell_{D^\ell}$.

Proof. SIC implies that the support of each of the finer elements in (12) intersects D^ℓ in at most one support component of $\zeta^\ell_{\mathbf{i}}$. □

Since the support components s of the ZP elements of level ℓ are contained in D^ℓ, the supports of the decoupled functions $\gamma^\ell_{\hat{\boldsymbol{\imath}}}$ are not entirely contained in $\Omega^{\ell+1}$.

We classify the decoupled functions according to the intersection of their supports with Ω^ℓ and $D^{\ell-1}$. We collect the functions with support contained in Ω^ℓ in the set

$$H^\ell = \{\gamma^\ell_{\hat{\boldsymbol{\imath}}} \mid \hat{\boldsymbol{\imath}} \in J^\ell\}, \text{ where } J^\ell = \{\hat{\boldsymbol{\imath}} \mid \operatorname{supp}^0 \gamma^\ell_{\hat{\boldsymbol{\imath}}} \subseteq \Omega^\ell\}. \tag{13}$$

The supports of the remaining functions intersect $D^{\ell-1}$. For each connected component $k \in S(D^{\ell-1})$, we collect the decoupled functions of level ℓ that take non-zero values there,

$$P_k^\ell = \{\gamma_{\hat{\boldsymbol{\imath}}}^\ell \mid \operatorname{supp}^0 \gamma_{\hat{\boldsymbol{\imath}}}^\ell \cap k \neq \emptyset\}.$$

The sets P_k^ℓ are mutually disjoint. Indeed, the supports of the ZP elements $\zeta_{\mathbf{i}}^\ell$ intersect at most one $k \in S(D^{\ell-1})$ due to SIC and $\operatorname{supp}^0 \gamma_{(\mathbf{i},s)}^\ell \subseteq \operatorname{supp}^0 \zeta_{\mathbf{i}}^\ell$.

For each connected component $k \in S(D^{\ell-1})$ we define the *partial chessboard* as the function

$$\pi_k^\ell(\mathbf{x}) = \sum_{\gamma_{\hat{\boldsymbol{\imath}}}^\ell \in P_k^\ell} \chi_{\hat{\boldsymbol{\imath}}} \gamma_{\hat{\boldsymbol{\imath}}}^\ell(\mathbf{x}), \tag{14}$$

where the coefficients $\chi_{\hat{\boldsymbol{\imath}}}$ are taken from the chessboard pattern defined in Section 2.

Lemma 14. *The supports of the partial chessboards π_k^ℓ, $k \in S(D^{\ell-1})$, are contained in Ω^ℓ.*

Proof. We rewrite Ω^ℓ as

$$\Omega^\ell = \Omega^0 \setminus D^{\ell-1} = \Omega^0 \setminus \bigcup_{k \in S(D^{\ell-1})} k.$$

Combining Lemma 13, $k \subseteq D^\ell$ and (5) confirms $\pi_k^\ell|_k = 0$, whereas $P_{k'}^\ell \cap P_k^\ell = \emptyset$ implies $\pi_k^\ell|_{k'} = 0$ for $k' \neq k$. □

Fig. 9 shows an adaptively refined triangulation and the supports (red and green regions) of the two partial chessboards of level 1 defined on it. The colored circles (blue/green and red/yellow, respectively) correspond to the decoupled functions in the sets P_k^1.

The definition of the sets H^ℓ uses the selection mechanism, which was introduced in Kraft (1997) to define a basis for hierarchical B–splines. We generalize this mechanism by applying it to decoupled functions and enriching the result with partial chessboards.

Definition 15. The set

$$H_+ = \bigcup_{\ell=0}^{N-1} \underbrace{H^\ell \cup \{\pi_k^\ell \mid k \in S(D^{\ell-1})\}}_{=H_+^\ell}, \tag{15}$$

is called the *enriched decoupled hierarchical generating system (EDHGS).*

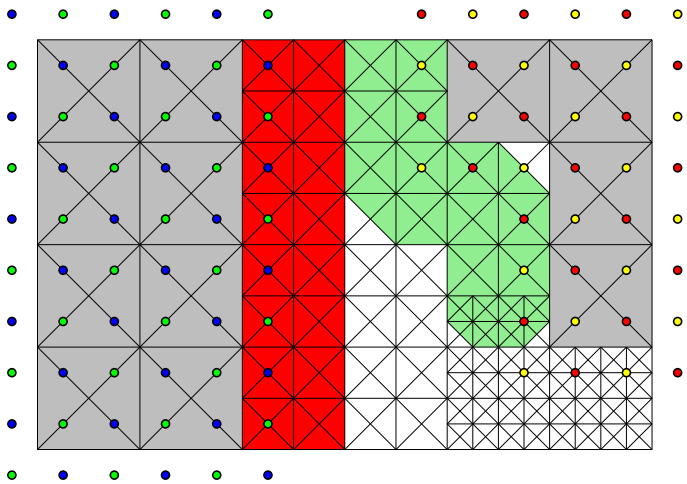

Figure 9: Two partial chessboards (supports and the coefficients of the involved decoupled functions) of level 1 on an adaptively refined triangulation with three levels. The two connected components $k \in S(D^0)$ are shown in gray.

It should be noted that the definition of EDHGS assumes SIC, since this assumption is needed for the definition of the partial chessboards.

Fig. 10 summarizes the relationships between the definitions in this section. The decoupled functions $\gamma^\ell_{\hat{\imath}} \in G^\ell$ are derived from the ZP elements $\zeta^\ell_{\mathbf{i}} \in Z^\ell$. They are then classified according to their supports, forming the sets P^ℓ_k and H^ℓ. The sets P^ℓ_k define partial chessboards. Finally, combining those with the selected functions H^ℓ provides the contribution H^ℓ_+ of each level to the EDHGS.

5. Completeness of EDHGS

We show that the enriched decoupled hierarchical generating system is complete, i.e., that it spans the entire hierarchical space defined in Section 3. We need to assume – in addition to SIC, which is required by the definition of the EDHGS – that the multicell domains D^ℓ are all admissible. This is equivalent to requiring that each connected component of Ω^ℓ contains at least one point on the boundary of Ω^0.

Theorem 16. *The EDHGS spans the entire multilevel spline space,* $\operatorname{span} H_+ = \mathbb{H}$, *if each difference set D^ℓ is an admissible multicell domain of level ℓ.*

Proof. The proof is inspired by that of Theorem 20 by Giannelli and Jüttler (2013). The EDHGS, however, is not linearly independent, thus the original proof does not apply directly.

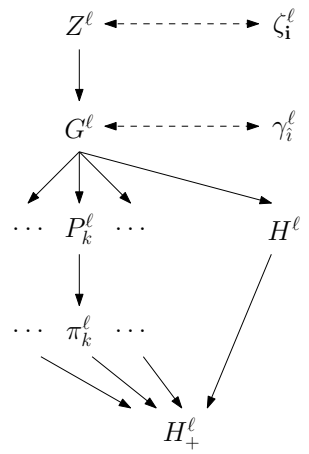

Figure 10: Graphical summary of the construction of the EDHGS.

On the one hand, $\operatorname{span} H_+ \subseteq \mathbb{H}$, as all the functions in H_+ are elements of $\mathbb{H}$ as well. On the other hand, we consider any $\sigma \in \mathbb{H}$ and show that it is contained in $\operatorname{span} H_+$.

We start by considering the restriction $\sigma^0 = \sigma|_{D^0}$, which is an element of the spline space $\mathbb{S}^1_2(\Delta^0)$. According to Theorem 8 and Lemma 13 it can be written as

$$\sigma^0 = \sum_{\hat{\boldsymbol{\imath}} \in I^0_{D^0}} \alpha^0_{\hat{\boldsymbol{\imath}}} \gamma^0_{\hat{\boldsymbol{\imath}}}|_{D^0} = \sum_{\hat{\boldsymbol{\imath}} \in J^0} \alpha^0_{\hat{\boldsymbol{\imath}}} \gamma^0_{\hat{\boldsymbol{\imath}}}|_{D^0} \in \operatorname{span} H^0_+,$$

with certain coefficients $\alpha^0_{\hat{\boldsymbol{\imath}}}$, since $I^0_{D^0} = J^0$, cf. (13).

We now consider the remainder

$$\sigma^1 = \left(\sigma - \sum_{\hat{\boldsymbol{\imath}} \in J^0} \alpha_{\hat{\boldsymbol{\imath}}} \gamma^0_{\hat{\boldsymbol{\imath}}} \right) |_{D^1},$$

which belongs to the spline space $\mathbb{S}^1_2(\Delta^1)$. Invoking Theorem 8 and Lemma 13 again, we obtain the representation

$$\sigma^1 = \sum_{\hat{\boldsymbol{\imath}} \in I^1_{D^1}} \alpha^1_{\hat{\boldsymbol{\imath}}} \gamma^1_{\hat{\boldsymbol{\imath}}}|_{D^1}, \tag{16}$$

with certain coefficients $\alpha^1_{\hat{\boldsymbol{\imath}}}$. Since

$$\sigma^1|_{D^0} = (\sigma - \sigma^0)|_{D^0}$$

is equal to zero on each connected component $k \in S(D^0)$, there exist scalars λ^1_k such that the coefficients satisfy $\alpha^1_{\hat{\boldsymbol{\imath}}} = \lambda^1_k \chi_{\hat{\boldsymbol{\imath}}}$ for all $\hat{\boldsymbol{\imath}} \in I^1_k$, due to Lemma 6. The

corresponding parts of the representation (16) can therefore be expressed by partial chessboards,

$$\sum_{\hat{\boldsymbol{\imath}} \in I_k^1} \alpha_{\hat{\boldsymbol{\imath}}}^1 \gamma_{\hat{\boldsymbol{\imath}}}^1 = \lambda_k^1 \pi_k^1.$$

We rewrite (16) as

$$\sigma^1 = \sum_{\hat{\boldsymbol{\imath}} \in J^1} \alpha_{\hat{\boldsymbol{\imath}}}^1 \gamma_{\hat{\boldsymbol{\imath}}}^1 |_{D^1} + \sum_{k \in S(D^0)} \lambda_k^1 \pi_k^1 |_{D^1} \in \operatorname{span} H_+^1. \tag{17}$$

Proceeding to the next level, we find a representation of

$$\sigma^2 = \left(\sigma - \sum_{\hat{\boldsymbol{\imath}} \in J^0} \alpha_{\hat{\boldsymbol{\imath}}}^0 \gamma_{\hat{\boldsymbol{\imath}}}^0 - \sum_{\hat{\boldsymbol{\imath}} \in J^1} \alpha_{\hat{\boldsymbol{\imath}}}^1 \gamma_{\hat{\boldsymbol{\imath}}}^1 - \sum_{k \in S(D^0)} \lambda_k^1 \pi_k^1 \right) |_{D^2} \in \operatorname{span} H_+^2,$$

and similarly for all higher levels $\ell = 3, \ldots, N-1$. In the final step we obtain a representation

$$\sigma^{N-1} = \left(\sigma - \underbrace{\sum_{\hat{\boldsymbol{\imath}} \in J^0} \alpha_{\hat{\boldsymbol{\imath}}}^0 \gamma_{\hat{\boldsymbol{\imath}}}^0}_{\in \operatorname{span} H_+^0} - \sum_{\ell=1}^{N-2} \underbrace{\left(\sum_{\hat{\boldsymbol{\imath}} \in J^\ell} \alpha_{\hat{\boldsymbol{\imath}}}^\ell \gamma_{\hat{\boldsymbol{\imath}}}^\ell + \sum_{k \in S(D^{\ell-1})} \lambda_k^\ell \pi_k^\ell \right)}_{\in \operatorname{span} H_+^\ell} \right) |_{D^{N-1}} \in \operatorname{span} H_+^{N-1}.$$

This completes the proof of $\sigma \in \operatorname{span} H_+$, since $D^{N-1} = \Omega^0$. □

Remark 17. If each difference set D^ℓ is connected, i.e., $|S(D^\ell)| \leq 1$, then the above theorem remains valid for the non-enriched decoupled hierarchical generating system $H = \bigcup_{\ell=0}^{N-1} H^\ell$ as well. Moreover, the theorem can be extended to non-enriched non-decoupled hierarchical generating systems by assuming a stronger version of SIC.

The assumption of Theorem 16 that each difference set D^ℓ is an admissible multicell domain implies that each Ω^ℓ is required to be connected to the boundary. This could be guaranteed by choosing a refinement strategy that always generates a thin stripe connecting the refined domain to the boundary. Thanks to the decoupling, it suffices to choose the width of this stripe as one cell of level ℓ. Fig. 11 (left) shows domains selected for refinement to level 1 and 2 (light and dark gray, respectively) as well as the stripes added to reach the boundary.

Finally, we present an example to show that the assumptions of Theorem 16 are indeed necessary for completeness of the EDHGS.

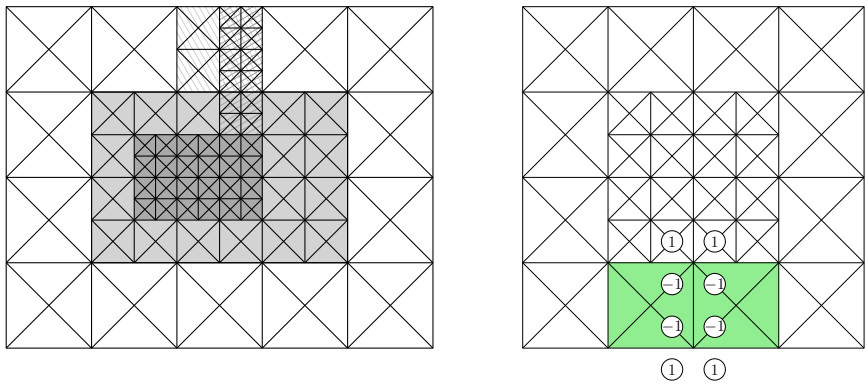

Figure 11: Left: areas selected for refinement together with their enlargement to ensure that the domain hierarchy is admissible. Right: Non-admissible mesh from Example 18.

Example 18. We consider the adaptively refined triangulation shown in Fig. 11 (right). The function, which is defined as the linear combination of the 8 ZP elements of level 1 with the coefficients specified in the picture, has been constructed by representing the function from Example 9 in the next finer level, using the refinement coefficients shown in Fig. 7. It clearly belongs to the multilevel spline space, since its restriction to Δ^0 is equal to the function from Example 9 and it also obviously belongs to $\mathbb{S}_2^1(\Delta^1)$, as it is a linear combination of level 1 ZP elements. However, it does not admit a representation with respect to the EDHGS, cf. Example 9. $\diamond$

Adding the function from this example to the EDHGS resolves the completeness problem in this specific case. We conjecture that this idea can be extended to more general configurations, thereby eliminating the assumption regarding the admissibility of the difference sets. A more detailed investigation of this issue is beyond the scope of the current paper.

6. Linear dependencies of the generating system

Any function $f \in \operatorname{span} H_+$ possesses a representation

$$f = \sum_{\ell=0}^{N-1} \left(\sum_{\hat{\boldsymbol{\imath}} \in J^\ell} d_{\hat{\boldsymbol{\imath}}}^\ell \gamma_{\hat{\boldsymbol{\imath}}}^\ell + \sum_{k \in S(D^{\ell-1})} p_k^\ell \pi_k^\ell \right), \tag{18}$$

where $(d_{\hat{\boldsymbol{\imath}}}^\ell)_{\hat{\boldsymbol{\imath}} \in J^\ell}$ and $(p_k^\ell)_{k \in S(D^{\ell-1})}$ are vectors of real coefficients and $S(D^{-1}) = \emptyset$.

A *linear dependency relation (LDR)* is a system of coefficients $(d_{\hat{\boldsymbol{\imath}}}^\ell)_{\hat{\boldsymbol{\imath}} \in J}$ and $(p_k^\ell)_{k \in S(D^{\ell-1})}$, $\ell = 0, \ldots, N-1$, such that the corresponding function f defined in (18) is equal to zero.

The LDRs form a linear space and we specify a basis for it; thus the linear dependencies of H_+ are well-controlled. One may see this in the terminology of operators: Equation (18) implicitly defines the *evaluation operator* $E : \mathbb{R}^{|H_+|} \to \mathbb{R}$, which can be applied to a system of coefficients. We provide a basis for $\ker(E)$.

Lemma 19. *The equation*

$$0 = \sum_{\{(\mathbf{i},s)\in J^\ell \mid s\subseteq k\}} \chi^\ell_{(\mathbf{i},s)}\gamma^\ell_{(\mathbf{i},s)} + \sum_{\{k'\in S(D^{\ell-1}) \mid k'\subseteq k\}} \pi^\ell_{k'}, \tag{19}$$

holds for each level ℓ and for each connected component $k \in S(D^\ell)$. Consequently, the associated system of coefficients (which are all equal to zero except for some coefficients of level ℓ) forms an LDR.

Proof. We use the definition of the partial chessboard (14) to rewrite the right-hand side of equation (19) as

$$\sum_{\{(\mathbf{i},s) \mid s\subset k\}} \chi^\ell_{\mathbf{i}}\gamma^\ell_{(\mathbf{i},s)}. \tag{20}$$

This sum involves all decoupled functions of level ℓ which take non-zero values on k and their coefficients form a chessboard pattern.

Firstly we consider its restriction to k. We rewrite it using (3) and Lemma 13 and obtain

$$\sum_{\{\mathbf{i} \mid \operatorname{supp}\zeta_{\mathbf{i}}\cap k\neq\emptyset\}} \chi^\ell_{\mathbf{i}}\zeta^\ell_{\mathbf{i}}, \tag{21}$$

which equals zero everywhere (on k) according to Lemma 6.

Secondly, considering the right-hand side (20) again for general arguments (i.e., also outside k), we express it in terms of ZP elements of the next finer level $\ell + 1$ using the refinement relation (11). This representation involves only ZP elements of level $\ell + 1$ with supports that intersect k, due to the definition of the decoupled functions (11) and the partial chessboards (14). The coefficients of these ZP functions of level $\ell+1$, however, are obtained by refining the chessboard pattern (21), and this is known to produce zero coefficients only (Zore and Jüttler, 2014, Example 22). This completes the proof. □

The equations in Lemma 19 are instances of evaluations of linearly independent LDRs. The linear independence is obvious since the equations involve mutually disjoint sets of coefficients. We will refer to them as Linear Dependency Generators (LDGs).

An example for LDGs of level $\ell = 1$ is shown in Fig. 12. Two such LDGs are obtained in this case, since $S(D^1)$ possesses two connected components (shown in

gray). The LDG on the left connected component involves two partial chessboards (visualized by the red dots that represent the participating decoupled functions) and 76 decoupled functions (represented by blue dots). The other LDG involves 48 decoupled functions (represented by green dots) but no partial chessboard. In total, we get two LDGs of level 0 (each involving 18 decoupled functions but no partial chessboard), two of level 1 and one of level 2 (involving two partial chessboards and 88 decoupled functions) in this situation.

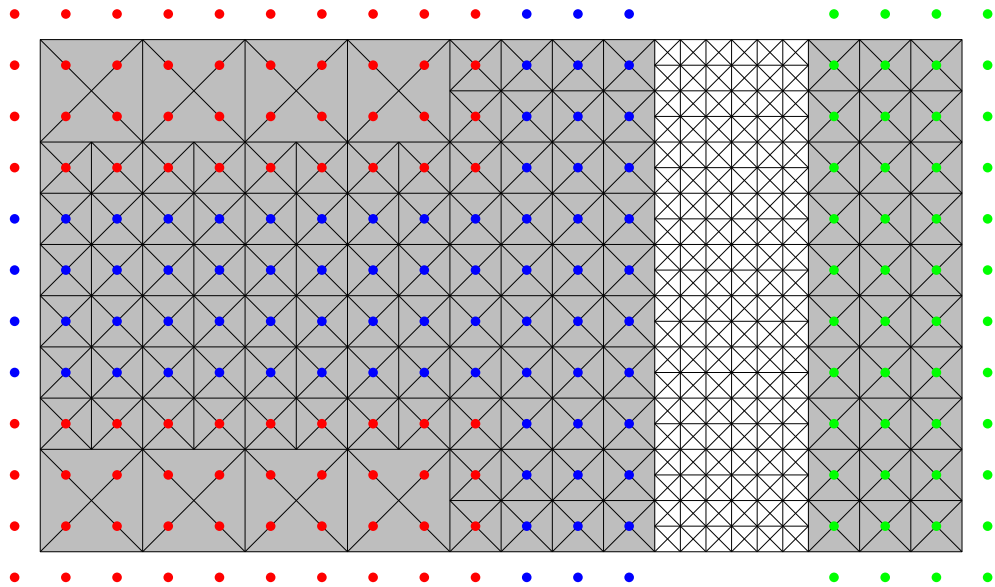

Figure 12: Linear dependency generators (LDGs) of level 1 on an instance of an adaptively refined criss-cross triangulation.

We show that the system of LDGs from Lemma 19 forms a basis of the space of LDRs. Consequently, the number of LDRs equals

$$\dim \ker(E) = \sum_{\ell=0}^{N-1} |S(D^\ell)|.$$

It should be noted that the definition of the EDHGS assumes that SIC is satisfied.

Theorem 20. *Any LDR that is present in the EDHGS is a linear combination of the LDGs in Lemma 19.*

Proof. We consider an LDR $f = 0$, where f is defined in (18), and re-arrange the sum according to the levels ℓ and the connected components of D^ℓ,

$$0 = \sum_{\ell=0}^{N-1} \sum_{k \in S(D^\ell)} \left(\sum_{(\mathbf{i},s) \in J^\ell, s \subseteq k} d^\ell_{(\mathbf{i},s)} \gamma^\ell_{(\mathbf{i},s)} + \sum_{k' \in S(D^{\ell-1}), k' \subseteq k} p^\ell_{k'} \pi^\ell_{k'} \right). \tag{22}$$

Note that the index sets of the sums within the brackets for different values of ℓ, k are mutually disjoint, since we assume SIC.

For $\ell = 0$ and the first connected component k, the only functions that are active on k are the decoupled functions $\gamma^0_{(\mathbf{i},s)}$ with indices satisfying $(\mathbf{i}, s) \in J^0, s \subseteq k$, but no partial chessboards. Invoking Lemma 6 confirms that the associated coefficients are a multiple of the corresponding LDG.

We now continue by considering the levels ℓ from 0 to $N-1$ and visiting one connected component k after the other. In each step we prove that the associated coefficients are a multiple of the corresponding LDG. This is possible since the coefficients of the previously considered decoupled functions and partial chessboards have been chosen so that their sum is equal to zero (as they are linear combinations of LDGs) and the supports of the remaining decoupled functions and partial chessboards do not intersect k.

Consequently, the only functions that are active on k are the decoupled functions $\gamma^\ell_{(\mathbf{i},s)}$ with indices satisfying $(\mathbf{i}, s) \in J^\ell, s \subseteq k$, and the partial chessboards $\pi^\ell_{k'}$ with indices $k' \in S(D^{\ell-1}), k' \subseteq k$. The latter ones can be split into decoupled functions according to (14). Invoking Lemma 6 again confirms that the associated coefficients are a multiple of the corresponding LDG. □

Corollary 21. *The dimension of the multilevel spline space $\mathbb{H}$ equals*

$$\dim \mathbb{H} = |H_+| - \sum_{\ell=0}^{N-1} |S(D^\ell)|$$

if each ring D^ℓ is an admissible multicell domain of level ℓ. A basis of $\mathbb{H}$ is obtained by removing one of the functions involved in each of the LDGs from H_+.

Under the assumptions of the previous corollary,

$$\dim \mathbb{H} = \sum_{\ell=0}^{N-1} |H^\ell| - S(\Omega^0).$$

In particular, this agrees with the observation that there is exactly one LDR among the separated functions of one level on a simply connected domain.

7. Conclusions

We defined the enriched decoupled hierarchical generating system (EDHGS) of ZP elements on adaptively refined criss-cross triangulations. The definition assumes that the subdomains – which represent the regions selected for refinement to a certain level – are chosen such that the resulting difference sets satisfy SIC. This assumption can be ensured by always refining sufficiently wide subdomains.

The completeness of the EDHGS was proved under an additional assumption. More precisely, the difference sets need to be admissible. This condition is fulfilled if each component of the refined area is connected to the boundary of the domain.

In addition, we studied the linear dependencies that are present in the EDHGS. They can be controlled easily and linear independence can be restored by simply eliminating one of the functions involved in each of the linear dependency generators, which have been identified. Combining this with the completeness result allows to compute the dimension of the multilevel spline space.

Future work may be devoted to the generalization of our approach to other classes of box splines.

Acknowledgments

Supported by the Austrian Science Fund (FWF, NFN S117 "Geometry + Simulation") and by the Seventh Framework Programme of the EU (projects EXAMPLE, GA No. 324340, and INSIST, GA No. 289361).

References

Aigner, M., Gonzalez-Vega, L., Jüttler, B. and Sampoli, M. L. (2009). Computing isophotes on free-form surfaces based on support function approximation, *Mathematics of Surfaces XIII*, pp. 1–18.

Bastl, B., Jüttler, B., Kosinka, J. and Lávička, M. (2010). Volumes with piecewise quadratic medial surface transforms: Computation of boundaries and trimmed offsets, *Comput. Aided Design* **42**: 671–679.

Bastl, B., Jüttler, B., Lávička, M. and Kosinka, J. (2008). Computing exact rational offsets of quadratic triangular Bézier surface patches, *Comput. Aided Design* **40**: 197–209.

Berdinsky, D., Kim, T.-W., Bracco, C., Cho, D., Mourrain, B., Oh, M. and Kiatpanichgij, S. (2014). Dimensions and bases of hierarchical tensor-product splines, *J. Comput. Appl. Math.* **257**: 86–104.

Berdinsky, D., Kim, T.-W., Cho, D., Bracco, C. and Kiatpanichgij, S. (2015). Bases of T-meshes and the refinement of hierarchical B-splines, *Comput. Methods Appl. Mech. Engrg.* **283**: 841–855.

Billera, L. J. (1988). Homology of smooth splines: generic triangulations and a conjecture of Strang, *Trans. Amer. Math. Soc.* **310**(1): 325–340.

Dagnino, C. and Lamberti, P. (2001). On the approximation power of bivariate quadratic c^1 splines, *J. Comput. Appl. Math.* **131**(1): 321–332.

Dahmen, W. and Micchelli, C. A. (1984). On the optimal approximation rates for criss-cross finite element spaces, *J. Comput. Appl. Math.* **10**(3): 255–273.

de Boor, C., Höllig, K. and Riemenschneider, S. (1993). *Box splines*, Springer–Verlag.

Deng, J., Chen, F., Li, X., Hu, C., Tong, W., Yang, Z. and Feng, Y. (2008). Polynomial splines over hierarchical T-meshes, *Graph. Models* **70**: 76–86.

Dokken, T., Lyche, T. and Pettersen, K. F. (2013). Polynomial splines over locally refined box–partitions, *Comput. Aided Geom. Design* **30**: 331–356.

Entezari, A., Nilchian, M. and Unser, M. (2012). A box spline calculus for the discretization of computed tomography reconstruction problems, *IEEE Trans. Medical Imaging* **31**(8): 1532–1541.

Forsey, D. R. and Bartels, R. H. (1988). Hierarchical B-spline refinement, *Comput. Graphics* **22**: 205–212.

Foucher, F. and Sablonnière, P. (2008). Approximating partial derivatives of first and second order by quadratic spline quasi-interpolants on uniform meshes, *Math. Comput. Simulation* **77**(2-3): 202–208.

Giannelli, C. and Jüttler, B. (2013). Bases and dimensions of bivariate hierarchical tensor–product splines, *J. Comput. Appl. Math.* **239**: 162–178.

Giannelli, C., Jüttler, B. and Speleers, H. (2012). THB–splines: The truncated basis for hierarchical splines, *Comput. Aided Geom. Design* **29**: 485–498.

Greiner, G. and Hormann, K. (1997). Interpolating and approximating scattered 3D-data with hierarchical tensor product B-splines, *in* A. L. Méhauté, C. Rabut and L. L. Schumaker (eds), *Surface Fitting and Multiresolution Methods*, Innovations in Applied Mathematics, Vanderbilt University Press, Nashville, TN, pp. 163–172.

Huang, Z., Deng, J., Feng, Y. and Chen, F. (2006). New proof of dimension formula of spline spaces over T-meshes via smoothing cofactors, *J. Comput. Math.* **24**(4): 501–514.

Kang, H., Chen, F. and Deng, J. (2014). Hierarchical B-splines on regular triangular partitions, *Graph. Models* **76**(5): 289–300.

Kiss, G., Giannelli, C., Zore, U., Jüttler, B., Großmann, D. and Barner, J. (2014). Adaptive CAD model (re-) construction with THB-splines, *Graph. Models* **76**(5): 273 – 288.

Kraft, R. (1997). Adaptive and linearly independent multilevel B–splines, *in* A. Le Méhauté, C. Rabut and L. L. Schumaker (eds), *Surface Fitting and Multiresolution Methods*, Vanderbilt University Press, Nashville, pp. 209–218.

Lai, M.-J. and Schumaker, L. L. (2007). *Spline Functions on Triangulations*, Cambridge University Press.

Lyche, T., Manni, C. and Sablonnière, P. (2008). Quasi-interpolation projectors for box splines, *J. Comput. Appl. Math.* **221**(2): 416–429.

Mokriš, D. and Jüttler, B. (2014). TDHB-splines: The truncated decoupled basis of hierarchical tensor-product splines, *Comput. Aided Geom. Design* **31**: 531–544.

Mokriš, D., Jüttler, B. and Giannelli, C. (2014). On the completeness of hierarchical tensor-product B-splines, *J. Comput. Appl. Math.* **271**: 53–70.

Mourrain, B. (2014). On the dimension of spline spaces on planar T–meshes, *Math. Comp.* **83**(286): 847–871.

Richter, M. (1998). Use of box splines in computer tomography, *Computing* **61**(2): 133–150.

Schenck, H. and Stillman, M. (1997). Local cohomology of bivariate splines, *J. Pure Appl. Algebra* **117**: 535–548.

Schillinger, D., Dedé, L., Scott, M. A., Evans, J. A., Borden, M. J., Rank, E. and Hughes, T. J. R. (2012). An isogeometric design-through-analysis methodology based on adaptive hierarchical refinement of NURBS, immersed boundary methods, and T-spline CAD surfaces, *Comput. Methods Appl. Mech. Engrg.* **249**: 116 – 150.

Sederberg, T. W., Zheng, J., Bakenov, A. and Nasri, A. (2003). T-splines and T-NURCCS, *ACM Trans. Graphics* **22**: 477–484.

Speleers, H., Dierckx, P. and Vandewalle, S. (2009). Quasi–hierarchical Powell–Sabin B–splines, *Comput. Aided Geom. Design* **26**: 174–191.

Speleers, H. and Manni, C. (2016). Effortless quasi-interpolation in hierarchical spaces, *Numer. Math.* **132**(1): 155–184.

Vuong, A.-V., Giannelli, C., Jüttler, B. and Simeon, B. (2011). A hierarchical approach to adaptive local refinement in isogeometric analysis, *Comput. Methods Appl. Mech. Engrg.* **200**: 3554–3567.

Wang, R. H. (2001). *Multivariate Spline Functions and Their Applications*, Kluwer, Dordrecht.

Yvart, A., Hahmann, S. and Bonneau, G.-P. (2005). Hierarchical triangular splines, *ACM Trans. Graphics* **24**: 1374–1391.

Zeng, C., Deng, F., Li, X. and Deng, J. (2015). Dimensions of biquadratic and bicubic spline spaces over hierarchical T-meshes, *J. Comput. Appl. Math.* **287**: 162–178.

Zore, U. and Jüttler, B. (2014). Adaptively refined multilevel spline spaces from generating systems, *Comput. Aided Geom. Design* **31**: 545–566.

Zwart, P. B. (1973). Multivariate splines with nondegenerate partitions, *SIAM J. Numer. Anal.* **10**(4): 665–673.